Supporting Information

Bismuth Drives the Morphology and Piezoresistivity of Lead-free $(TMSO)_3Sn_{3x}Bi_{2(1-x)}I_9$ Halide Perovskite thin films

Simone Virga,[a] Giuseppe Arrabito,[a] Vittorio Ferrara,[a] Michelangelo Scopelliti,[a] Alessandro Longo,[b] Bruno Pignataro,*[a] and Francesco Giannici*[a]

a. Dipartimento di Fisica e Chimica "Emilio Segrè", Università degli Studi di Palermo, Viale delle Scienze, 90128 Palermo, Italy. E-mail: bruno.pignataro@unipa.it; francesco.giannici@unipa.it

b. European Synchrotron Radiation Facility, 71, avenue des Martyrs, CS 40220, 38043 Grenoble Cedex 9, France and Consiglio Nazionale delle Ricerche, ISMN-CNR, I-90146 Palermo, Italy.

Table S1. Reagents used for each synthesis and their respective labels.

Label	Formula	$TMSO^+$ mmol	Sn^{2+} mmol	Bi^{3+} mmol
Bi0	$(TMSO)SnI_3$	1	1	--
Bi25	$(TMSO)_3Sn_{3x}Bi_{2(1-x)}I_9$	1	0.75	0.25
Bi50	$(TMSO)_3Sn_{3x}Bi_{2(1-x)}I_9$	1	0.5	0.5
Bi75	$(TMSO)_3Sn_{3x}Bi_{2(1-x)}I_9$	1	0.25	0.75
Bi100	$(TMSO)_3Bi_2I_9$	1	--	1

Fig. S1 Rietveld refinement plots for $(TMSO)SnI_3$ (Bi0). Observed and calculated traces in blue and red, respectively, with the difference plot (in cyan) and peak markers (blue bars) at the bottom.

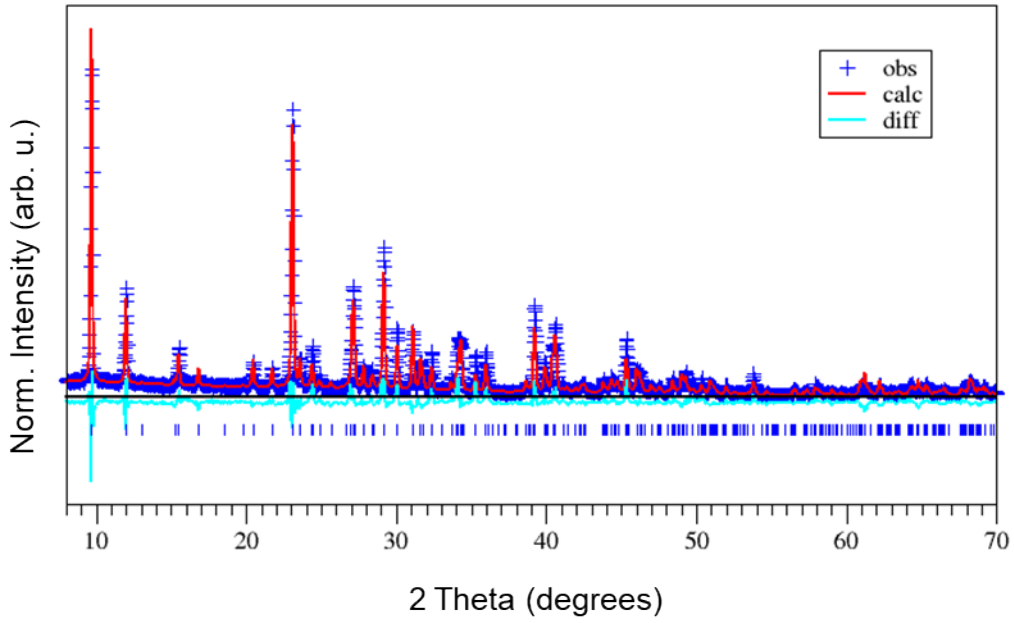

Fig. S2 Rietveld refinement plots for $(TMSO)_3Bi_2I_9$ (Bi100). Observed and calculated traces in blue and red, respectively, with the difference plot (in cyan) and peak markers (blue bars) at the bottom.

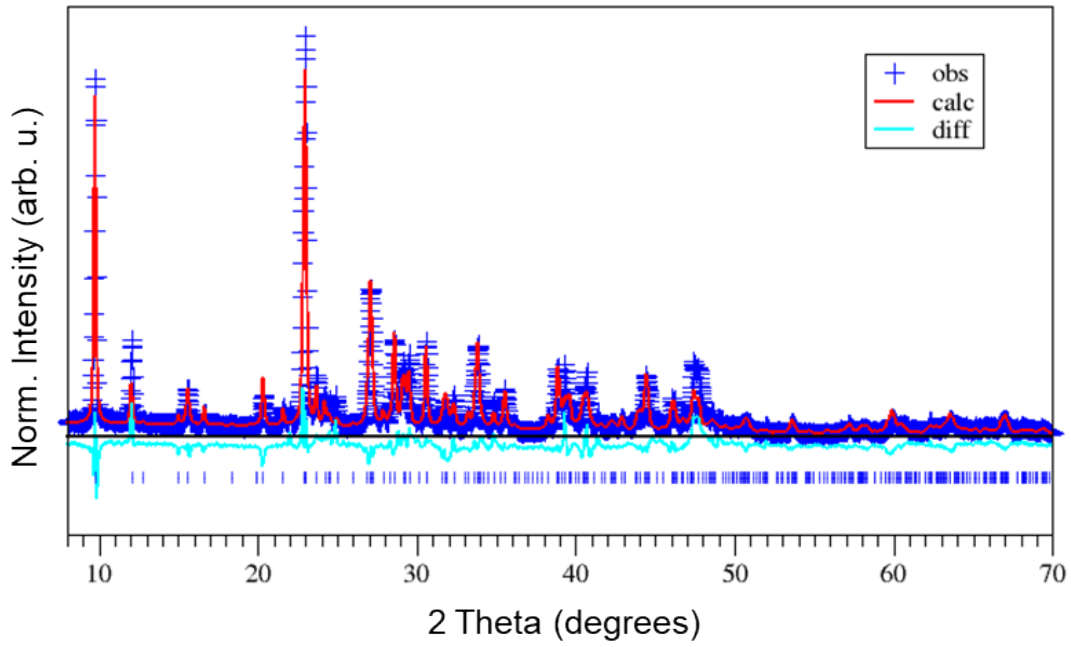

Fig. S3 Rietveld refinement plot for Bi25. Observed and calculated traces in blue and red, respectively, with the difference plot (in cyan) and peak markers (blue bars) at the bottom.

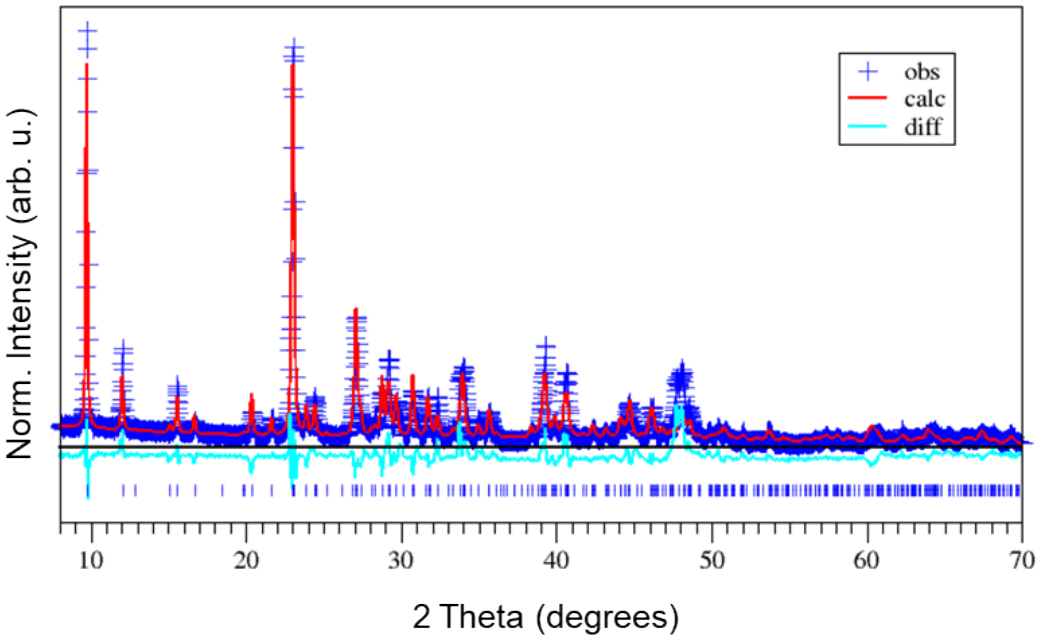

Fig. S4 Rietveld refinement plot for Bi50. Observed and calculated traces in blue and red, respectively, with the difference plot (in cyan) and peak markers (blue bars) at the bottom.

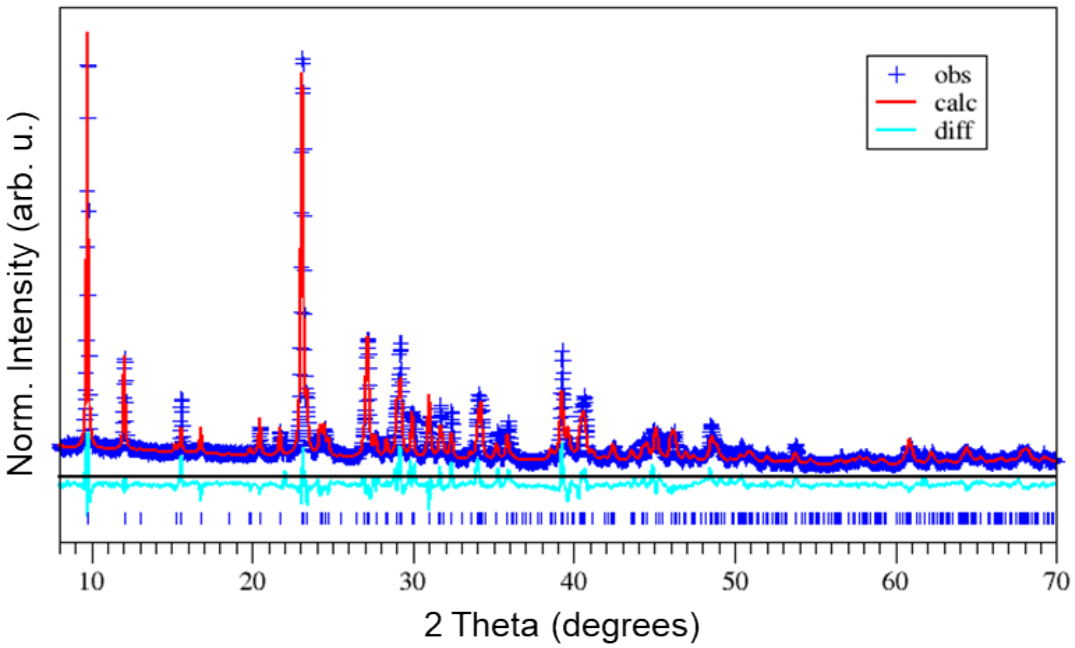

Fig. S5 Rietveld refinement plot for Bi75. Observed and calculated traces in blue and red, respectively, with the difference plot (in cyan) and peak markers (blue bars) at the bottom.

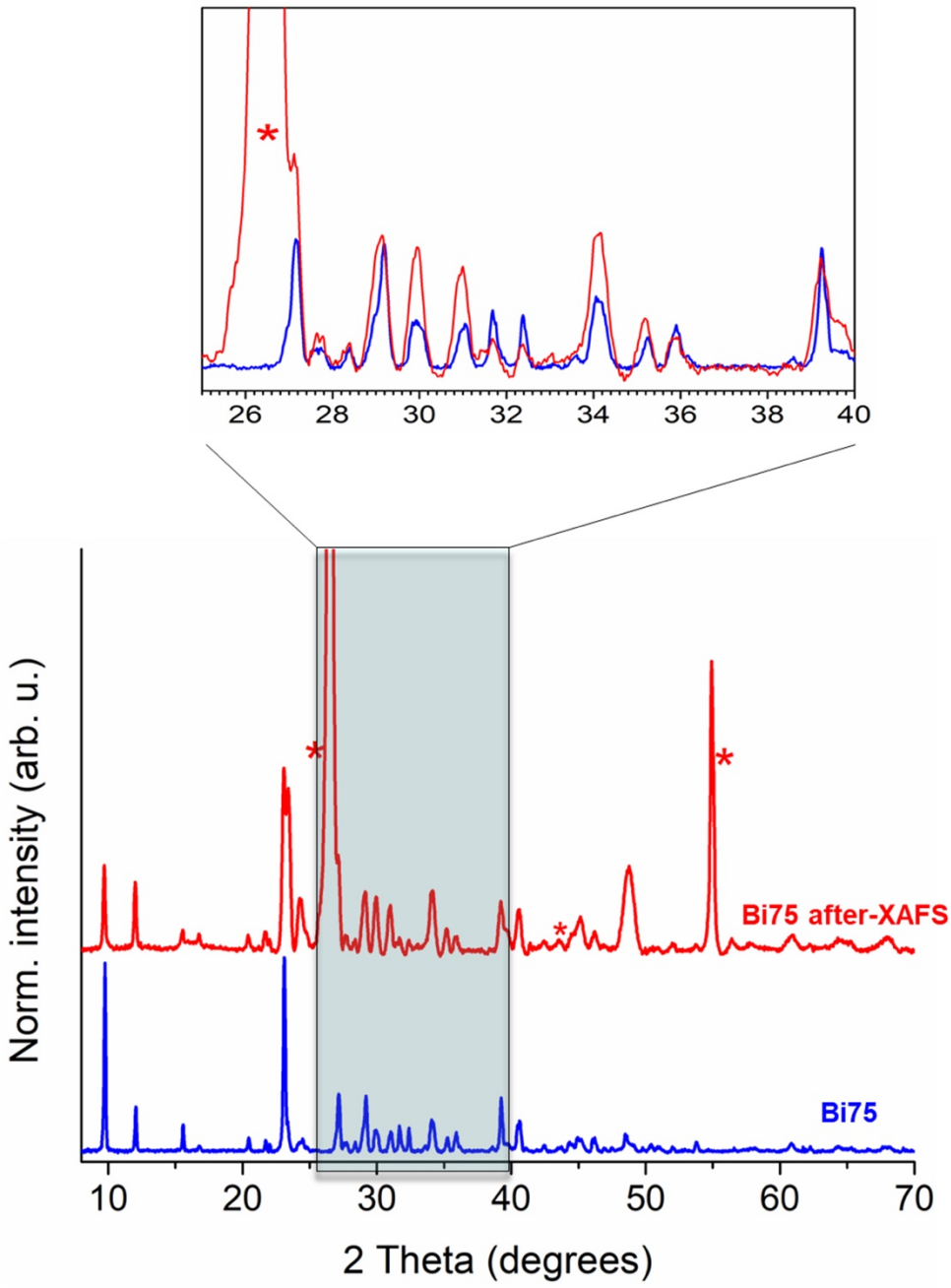

Fig. S6 Diffraction data of Bi75 pre (blue) and after (red) XAFS with an enlargement of the 25−40° section, where the consistency of the peaks position is more evident. A red asterisk marks Bragg peaks due to the boron nitride dilutant.

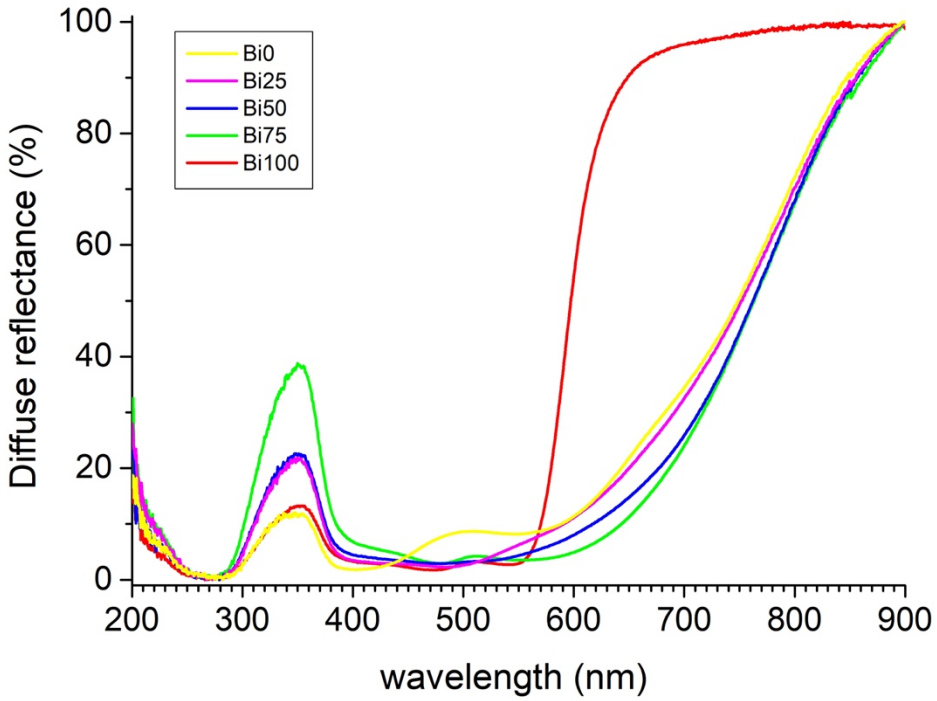

Fig. S7 UV-vis-NIR reflectance spectra of all samples as bulk powders.

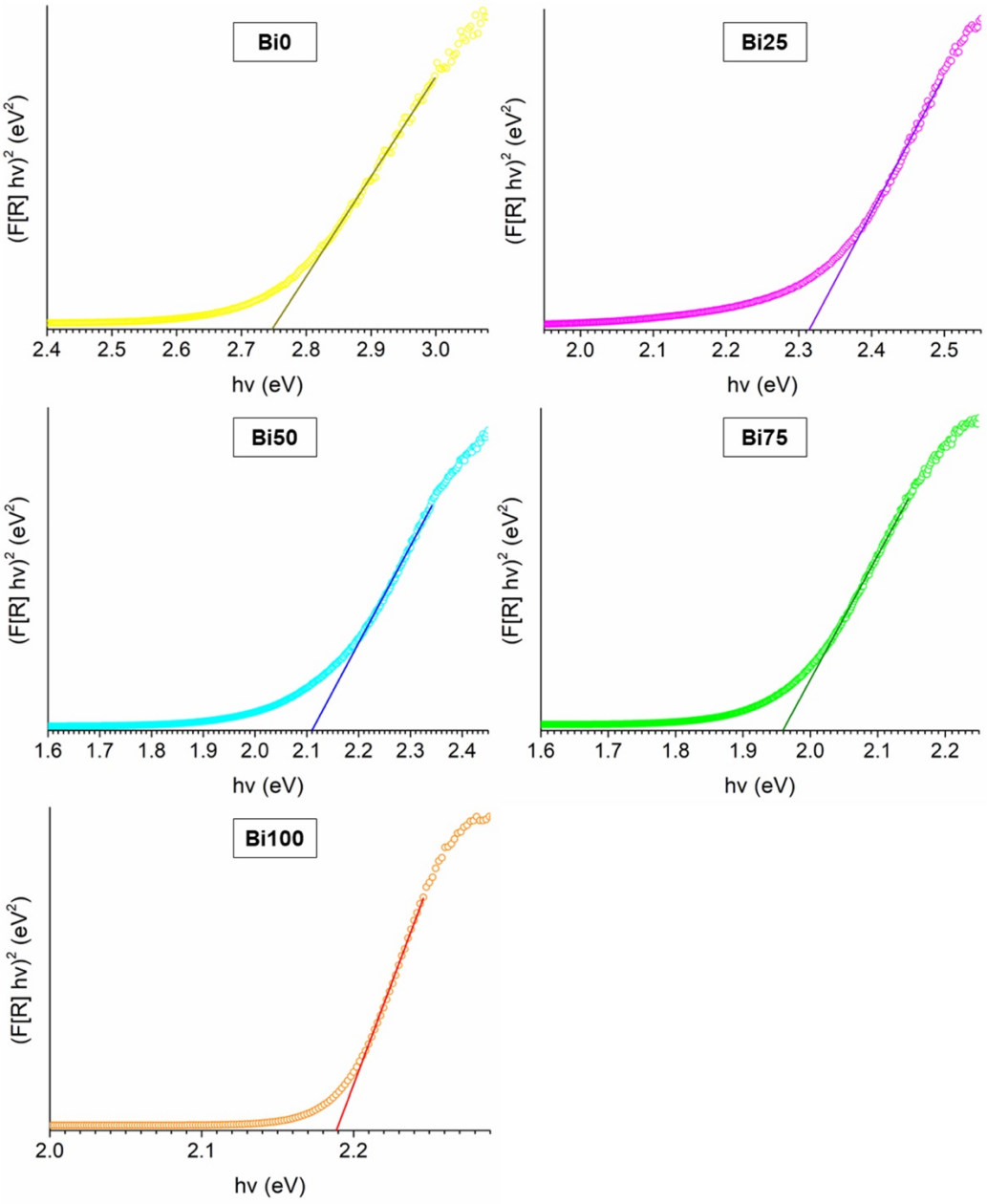

Fig. S8 Tauc Plots of the powders of (a) $(TMSO)SnI_3$, (b-d) $(TMSO)_3Sn_{3x}Bi_{2(1-x)}I_9$ ($0 \leq x \leq 1$), and (e) $(TMSO)_3Bi_2I_9$.

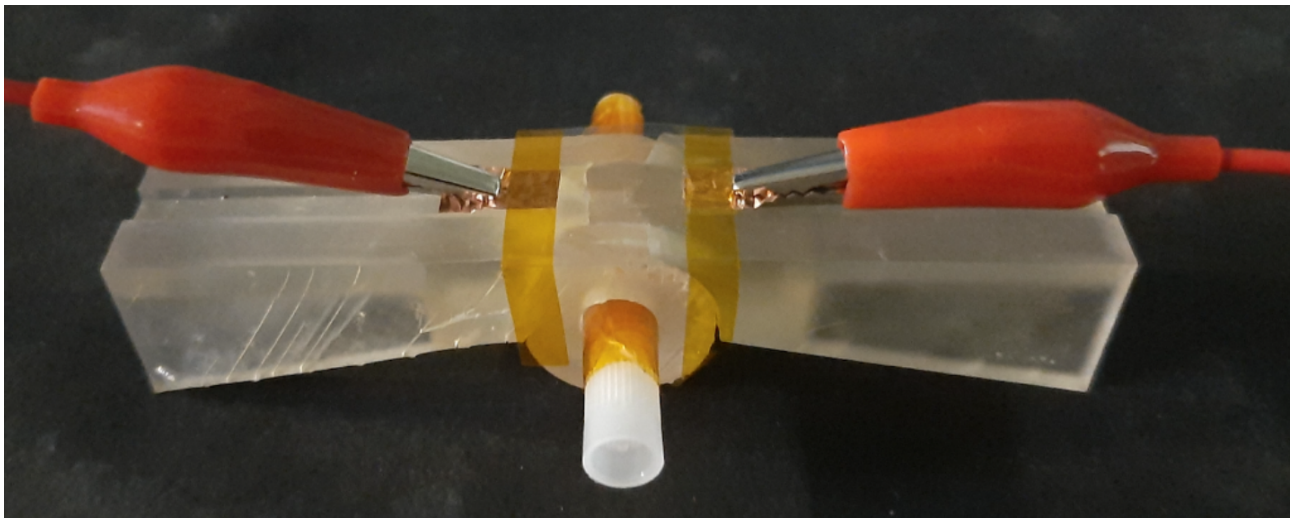

Fig. S9 Optical photograph of the piezoresistive sensor mounted on the bending device.

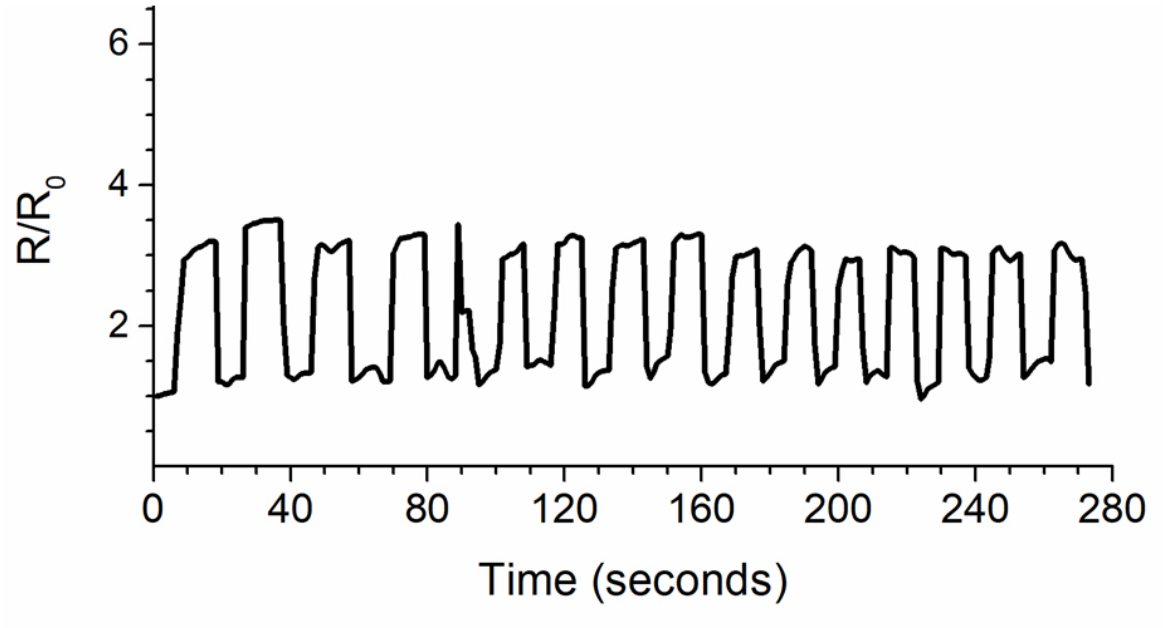

Fig. S10 Electrical resistance response of multicycle 0-90° bending of the Bi75 sample.

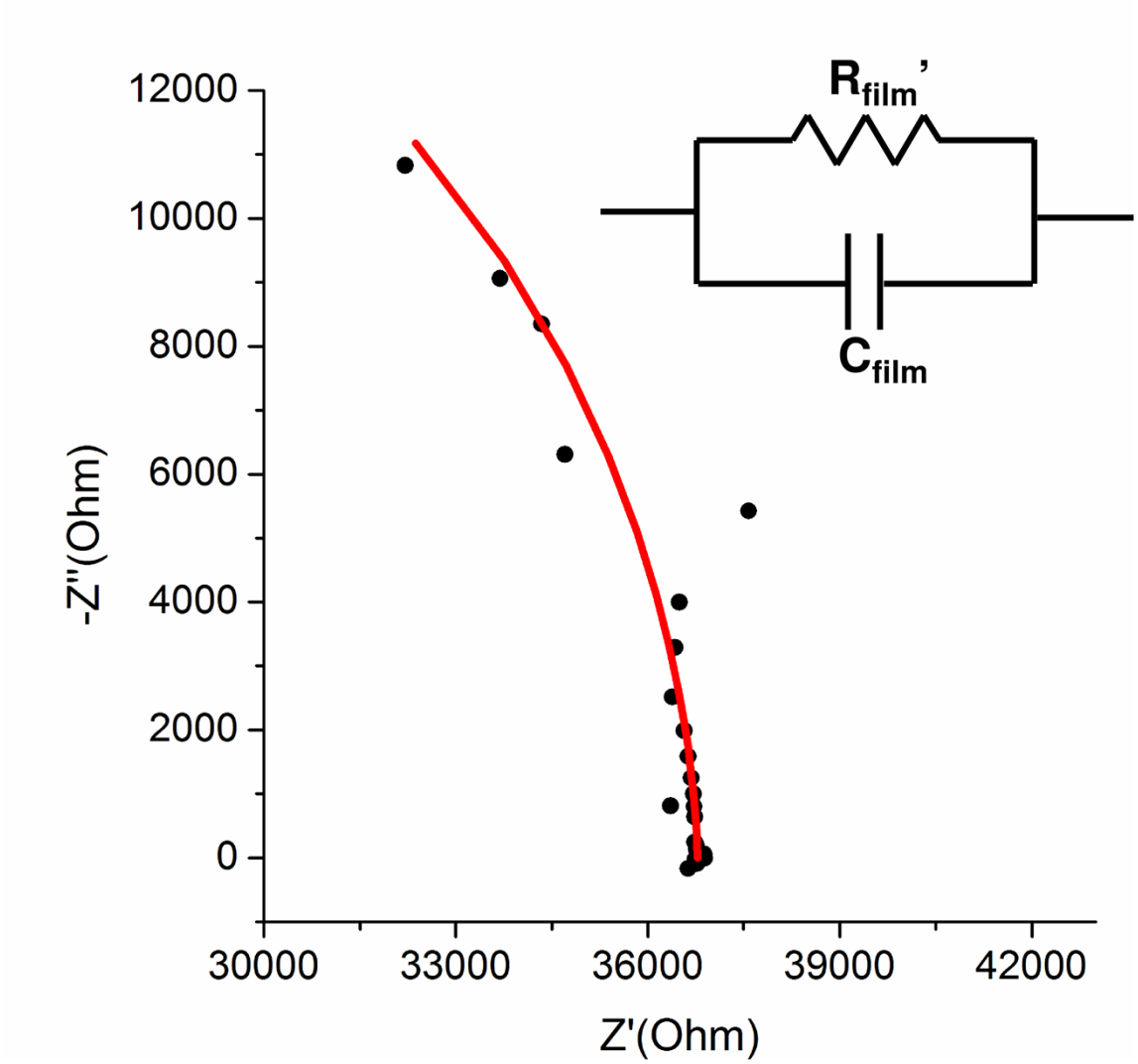

Fig. S11 Nyquist plots and relative fits of Bi75 bending after 0°-90°-0° bending cycles reporting the best fits for model circuit 2.